

Ring Opening of Methylcyclopentane on Alumina-Supported Rh Catalysts of Different Metal Loadings

D. Teschner, K. Matusek, and Z. Paál

Institute of Isotope and Surface Chemistry, Chemical Research Center, Hungarian Academy of Sciences, P.O.B. 77, H-1525 Budapest, Hungary
E-mail: paal@iserv.iki.kfki.hu

Received October 15, 1999; revised January 13, 2000; accepted January 17, 2000

Hydrogenolytic ring opening of methylcyclopentane (MCP) was investigated on Rh/Al₂O₃ catalysts, prepared by the incipient wetness method. The catalysts, with different metal loadings (0.3%, 3%, and 10%) and altered reduction temperatures (573 K, LTR; 973 K, HTR), were further characterized by temperature-programmed reduction (TPR). With high metal loading (10Rh) we observed a second TPR peak, which appeared after the impregnated as well as the subsequently oxidized form was reduced. This second peak was absent with 0.3 and 3% Rh/Al₂O₃. Strong dependence could be seen in the distribution of ring-opening products as a function of temperature and hydrogen pressure with 10Rh and 3RhHTR. We attribute these variations to changing selectivities toward fragmentation. This selectivity varies with the reaction temperature, hydrogen pressure, and catalyst preparation. Another behavior pattern appeared with 0.3Rh and 3RhLTR, exhibiting no selectivity variation in the ring-opening product distribution. This was caused by the random fragment production from the ring-opening surface species. We compared the ring-opening distribution with the fragmentation pattern and found correlation in the case of the first type of catalysts and suggest a common active site on Rh/alumina for the two main reactions, single and multiple C–C bond rupture, respectively. Due to the parallel variation in catalytic and TPR behavior of Rh/Al₂O₃, we attribute the variations in reaction mechanisms to changes in metal loadings and pretreatments, leading to different particle morphologies. By changing the metal loading and altering the reduction temperature, we suggest two forms of rhodium based on (i) temperature-programmed reduction study and (ii) the behavior of different samples in MCP reactions. © 2000 Academic Press

Key Words: Rh/Al₂O₃; TPR; methylcyclopentane ring opening; fragmentation.

INTRODUCTION

In the late 70s comparative studies of several metals in the reactions of C₆ hydrocarbons were performed to classify the catalytic properties of the transition metals. It has been found that four metals, Ir, Pt, Pd, and Rh, were able to catalyze in C₅ cyclization of the alkane reactant; at the same time, under proper conditions, methylcyclopentane (MCP) produced mainly C₆ alkanes (1). The reaction of MCP over these metals was considered to be highly sensitive to the

catalyst structure and therefore may be a suitable model reaction to test various metal catalysts (1, 2).

The ring opening (RO) of alkylcyclopentanes, including MCP, can occur in a “selective” or “random” way in accordance with the probability of breaking C–C bonds in the C₅ ring (3–17). Kramer and Zuegg (4, 5) interpreted the observed particle size dependence of the ring-opening product distribution on supported Pt catalysts in terms of the non-selective mechanism occurring on “adlineation sites,” i.e., on ensembles at the metal–support borderline, whereas selective ring opening would involve pure metallic sites. The structure of the surface intermediate in selective ring opening has been strongly disputed: “edgewise” or “flat” geometries, in both cases “associative” or “dissociative” structures were proposed, the latter meaning on the degree of dehydrogenation of the surface intermediate (2, 6–8).

As opposed to Pt, rhodium behaves differently in skeletal reactions of cyclopentanes. Rhodium represented higher selectivity to open the C₅ ring in bissecondary positions. Counter claims appeared concerning the particle size dependence (9–11). Del Angel *et al.* (9) observed only a slight increase in the *n*-hexane (nH) selectivity from 2% to 8% with increasing dispersion over Rh/Al₂O₃ catalysts at 496 K. At the same time the *n*-hexane selectivity on Rh/silica varied between 1% and 3%. This implies that the MCP ring opening was strongly selective, even in the case of *D* = 100%. In addition, small rhodium particles on silica exhibited greater specific activity than large rhodium particles and the reverse trend was observed on alumina where large particles were more active. The variation of activity with rhodium dispersion was attributed to the ability of Al₂O₃ to stabilize the cubooctahedral morphology of small Rh particles. On SiO₂, the interaction between rhodium particles and support is weaker and the small particles may possess icosahedral structure. The aforementioned result indicates that the support plays a significant role in determining the abundance of various Rh crystal planes, hence, the catalytic properties of Rh particles.

In our previous study (12) we investigated the effect of support in MCP reaction over Rh/silica and Rh/alumina



and compared the relative importance of ring opening and fragmentation to single- and multiple-C–C bond rupture, respectively. We found that the support influences both (i) the ratio of the single- and multiple-bond(s) rupture, due to different H₂ pressure dependence, via different hydrogen spillover on SiO₂ and Al₂O₃, and (ii) the ring-opening product distribution at a given surface H coverage.

Kalakkad *et al.* (18) investigated the effect of metal loading on *n*-butane hydrogenolysis over Rh/alumina and Rh/silica and correlated it with single-crystal surface results. The selectivity of ethane formation on the highly dispersed rhodium, yielding 80% ethane, was different from that observed on low-index single-crystal surfaces of Rh. As the particle size increased, the selectivity of the catalysts approached the value of 50%, formed on Rh(111). They suggested particles with predominant Rh(111)-like surfaces as the particle diameter increased. Another good example for particle size effect was the conversion of 2,2,3,3-tetramethylbutane over Rh/alumina (14): the reactant gave iC₇ plus methane on small particles and much iC₄ on large particles.

Several research teams studied the effect of the oxidation/reduction treatments on the particle microstructure to establish correlation between activity and structure of supported Rh catalysts (11, 19–24). The catalytic performance of alumina-supported Rh was sensitive to the surface structure of the metal nanoparticle: “oxidation at 725 K followed by low-temperature reduction (LTR) at 525 K produced Rh particles with disordered (“rough”) surfaces; however, when oxidation was followed by high-temperature reduction (HTR) at 725 K, the low-Miller-index facets were stabilized” (22). High turnover frequencies were observed on catalysts containing mainly Rh particles with disordered surfaces. Fenoglio *et al.* (11) found a maximum in the activity of MCP hydrogenolysis at about 550 K as a function of the reduction temperature on silica- and titania-supported rhodium. This maximum was accompanied by a minimum in selectivity toward *n*-hexane.

Wong and McCabe (24) examined the morphology of silica-supported Rh catalysts by temperature-programmed oxidation and reduction (TPO, TPR) and transmission electron microscopy (TEM). They found evidence for two forms of Rh—a low-temperature oxidized/reduced form and a high-temperature oxidized/reduced form, the latter resembling bulk Rh in its oxidation/reduction behavior. These two forms of Rh were distinguished by their particle morphology. The low-temperature reduction form was associated with particles having crystal domains of ca. 6.0 nm or less which could exist either as segregated particles or as subunits of larger aggregates of crystallites. The high-temperature reduction form was associated with particles greater than 6.0 nm, exhibiting a high degree of crystallinity in microbeam electron diffraction.

Several studies concerning MCP ring opening on rhodium interpreted the reaction mechanism according to

what was found for Pt, although the particle size effect was different. Further, olefins were produced on Pt while a significant amount of fragments were observed on Rh. The negligible amount of olefins on Rh indicates that the degree of dehydrogenation of the surface intermediate should be different (independent of $p(\text{H}_2)$ and T). The present work reports on the reaction of MCP over alumina-supported Rh catalysts. The reaction was investigated under conditions (T , $p(\text{H}_2)$) permitting a large variation (5%–60%) of the fragmentation selectivity. Thus, we could compare single and multiple hydrogenolysis. The effect of metal loading and catalyst pretreatment on the reaction mechanism will also be discussed.

METHODS

Catalysts

Catalysts with 0.3%, 3%, and 10% Rh on an Al₂O₃ support (0.3Rh, 3Rh, and 10Rh, respectively) were prepared by wet impregnation of the support (Rhône-Poulenc, γ -Al₂O₃, 200 m² g⁻¹) with an aqueous solution of RhCl₃ · 3H₂O. The catalysts were dried overnight at 393 K and reduced in H₂ for 1 h either at 573 or 973 K (denoted as LTR and HTR, respectively).

The catalysts were characterized by temperature-programmed oxidation/reduction (TPO/TPR) and tested in catalytic reactions. The TPO/TPR experiments were carried out as described elsewhere (25). Reduction of the catalysts was carried out in a 10% H₂/Ar mixture and oxidation was carried out in a 10% O₂/He mixture. The heating rate was 20 K/min. Mass flow controllers were used to maintain the flow rate of the gas mixture at 20 cm³/min. The dispersion of rhodium was determined by H₂–O₂ titration—assuming a stoichiometry of H/Rh = 1 and O/Rh = 1—in the same apparatus. Although for small Rh clusters a different stoichiometry (H/Rh > 1) was suggested by Kip *et al.* (26), the likely experimental error using their values was less than 10%.

Reactions

Hydrogenolysis of MCP was used as a test reaction. The catalytic experiments were carried out in a closed-loop apparatus ($V = 155$ ml) connected to a CP 9001 gas chromatograph with a 50-m squalane-coated steel capillary column and a FID detector (12, 13). A standard MCP pressure of 10 Torr was used and the hydrogen pressure was varied between 120 and 480 Torr. The reaction temperatures ranged from 468 to 513 K. The sampling took place after 5 min. Regeneration between runs was carried out with 30 Torr air for 2 min followed by evacuation and 3 min of hydrogen treatment at 100 Torr. Methylcyclopentane (Merck, GC grade) contained traces of *n*-hexane, which was taken into account when the product composition was calculated. The turnover frequencies were calculated as the number of MCPs reacted

per one surface Rh atom per hour. Selectivities (*S*) were expressed as moles of MCP reacted rather than product moles. The term ring-opening product (ROP) refers to saturated C₆ products, while fragments (<C₆) to products containing less than six carbon atoms.

RESULTS

TPR

Three different catalysts have been used in the present study to investigate the effect of metal loading. Figure 1 depicts TPR profiles obtained on samples impregnated with RhCl₃. While the catalysts 0.3Rh and 3Rh show one peak with a slight, stretching shoulder on the high-temperature side, sample 10Rh has two overlapping peaks. Bulk reduction/oxidation of large particles always needed the most severe conditions. The well-dispersed precursor phase can be attached to the support via physisorption or by ion exchange. With more RhCl₃ · 3H₂O the relative quantity of the physisorbed part should have increased, so the interaction between precursor and support became, possibly, weaker. Thus, the reduction peak appeared at lower temperatures with higher loadings. The first peak in the case of 10Rh can, hence, be correlated with the single peak of the other two samples. The second band centered at about 500 K appeared with high metal loading only. This high-temperature peak can be assigned to a bulk reduction of the precursor phase. Similar shifts in the TPR pattern with metal loading and particle size and bulk assignment can be found in the literature (27–29).

After 1 h of reduction at 573 K we performed a TPO (terminated with an isothermal period at 873 K for 1 h)/TPR cycle. These second TPR patterns for the three catalysts are illustrated in Fig. 2. The peaks are generally shifted to a lower temperature by 20 K. Samples 3Rh and 10Rh have a main band at about 410 K and a minor peak remains from the high-temperature peak of 10Rh shown in Fig. 1.

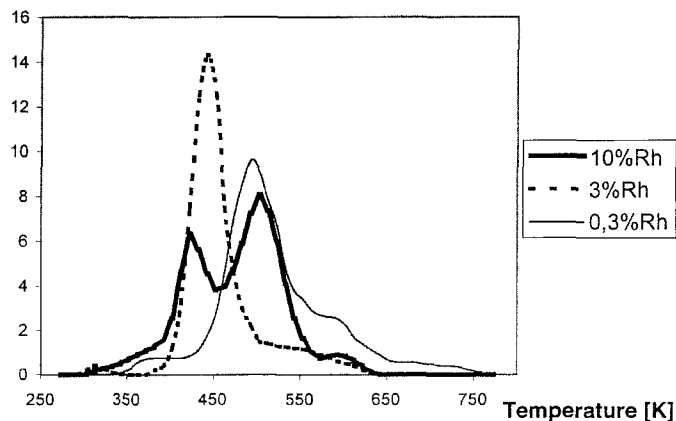


FIG. 1. Temperature-programmed reduction profiles for the impregnated samples.

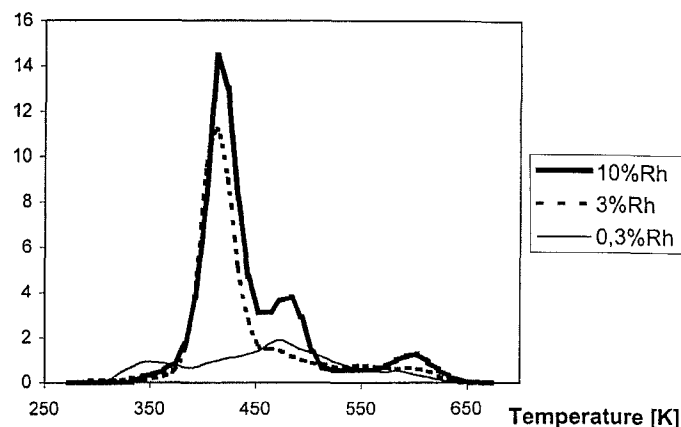


FIG. 2. Temperature-programmed reduction profiles after oxidation at 873 K.

Catalyst 0.3Rh has a continuous, stretching band, which can point to a strong interaction of the two oxide phases. This interaction manifests itself in a decreased hydrogen consumption compared to the first reduction. The value of this drop being 10%, 30%, and 70%, respectively, with 10%, 3%, and 0.3% metal loading. Thus, 2/3 of the Rh was not detectable in the second reduction with a 0.3% metal loading. Rh might have been embedded in the support (30, 31).

Dispersion values measured in the same apparatus after appropriate reduction are shown in Table 1. The values decreased with increasing metal loading.

Catalytic Tests

We investigated the catalytic properties of the three Rh/alumina catalysts subjected to two different

TABLE 1
Fragment Selectivities and Activation Energies
for the Various MCP Reactions

Samples	<i>T</i> ^a (K)	<i>D</i> (%)	<i>E</i> _a (RO) (kJ/mol)	<i>E</i> _a (<C ₆) (kJ/mol)	Reaction conditions		<i>S</i> (<C ₆)
					<i>T</i> ^b (K)	<i>P</i> (H ₂) (Torr)	
0.3RhLTR	573	57	34 ^c	79	468	480	16.5
					513	120	58.0
0.3RhHTR	973	67	24 ^c	70	468	480	10.1
					513	120	52.3
3RhLTR	573	25	50	71	468	480	18.0
					513	120	48.1
3RhHTR	973	32	26 ^c	58	468	480	4.5
					513	120	43.7
10RhLTR	573	18	44	110	468	480	4.2
					513	120	40.7
10RhHTR	973	18	33	79	468	480	3.8
					513	120	38.3

^a Reduction temperature.

^b Reaction temperature.

^c Activation energy for the lower temperature range (without the bending part of the plot) MCP = 10 Torr.

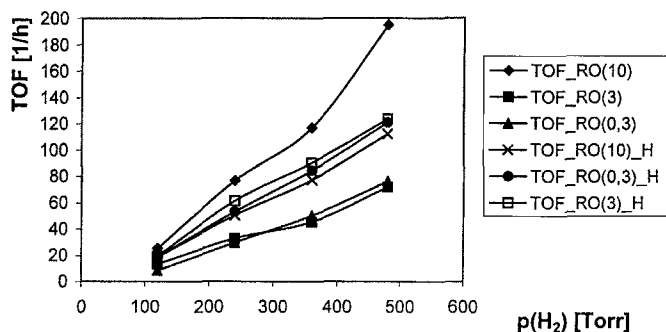


FIG. 3. Turnover frequencies for ring-opening products as a function of hydrogen pressure ($T = 513$ K). The metal content is given in parentheses; the added "H" suffix means HTR catalysts.

pretreatments by using the hydrogenolytic ring opening of methylcyclopentane as a test reaction. Ring-opening (C_6 alkanes) and hydrogenolysis products ($<C_6$ fragments) can be distinguished. No unsaturated hydrocarbons were detected. The selectivities did not change during longer runs up to $\sim 20\%$ conversion values. This means that secondary reactions were not important; thus, the product selectivities on different catalysts could be compared, even at different conversion levels. Selectivities and turnover frequencies (TOF) were determined at conversion values of 0.5–10%.

Figures 3 and 4 reveal the turnover frequencies of the two main reaction types as a function of the $p(H_2)$ for the different samples. The maximum rate of ring opening was reached at higher hydrogen pressure than any of the alkane reactions (2, 7, 32, 33). In the measured hydrogen pressure range, the TOF for the ring-opening reaction increased monotonically with $p(H_2)$, as shown in Fig. 3. However, clear variations can be seen if the metal loading and reduction temperature were changed. Sample 10RhLTR had the highest activity and the H_2 effect was also the most marked. Comparing its activity with that of 10RhHTR, it is seen that high-temperature reduction decreased the TOF when the metal loading was 10%. The reverse trend was seen with

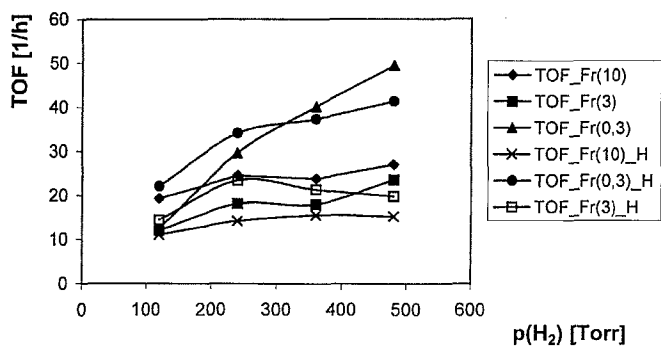


FIG. 4. Turnover frequencies for $<C_6$ fragments as a function of hydrogen pressure ($T = 513$ K). The metal content is given in parentheses; the added "H" suffix means HTR catalysts.

lower metal content: higher reduction temperature resulted in higher activity. The activity patterns for 0.3Rh and 3Rh were quite similar in the LTR states and in the HTR state at 513 K. This activity picture is in good agreement with the effect of particle size and pretreatment reported previously (9, 18, 20–23). With a 10% metal loading catalyst, subjected to low-temperature reduction, large Rh particles can be formed with corrugated flat morphology (18, 21), which was responsible for the high activity. This was also confirmed for Ru (34). Figure 4 shows the fragmentation activity; here, the two 0.3Rh catalysts showed the highest TOF. The H_2 effect was also the most pronounced here. The hydrogen pressure, hence, the surface hydrogen concentration (32), played no important role in determining the hydrogenolysis activity in the case of the other four catalysts. Apart from 0.3Rh, the $p(H_2)$ dependence was rather different for ring opening and fragmentation. This may point to the different degrees of dehydrogenation of the respective surface intermediates (2, 32).

Figure 5 depicts the relative importance of fragmentation compared to that of ring opening as a function of hydrogen pressure and temperature. The results for 3RhHTR are shown, but the tendencies are identical to the others. Higher temperature and lower $p(H_2)$ shifted the MCP hydrogenolysis toward multiple-C–C bond cleavage. The temperature effect is evident considering the further loosening of chemical bonds at higher temperature. The influence of hydrogen, which is opposite to what one could expect on the basis of the reaction stoichiometry, indicates again a different dehydrogenation of the reactant on the surface. Table 1 gives the highest and lowest fragment selectivities observed for each catalyst. The hydrogenolysis selectivity decreased with increasing metal loading. The lowest $S(<C_6)$ for samples 0.3Rh and 3RhLTR was more than twice as high than those of the other catalysts, and a slight difference can still be seen in the highest values as well. High-temperature reduction lowered the fragment selectivity in every case.

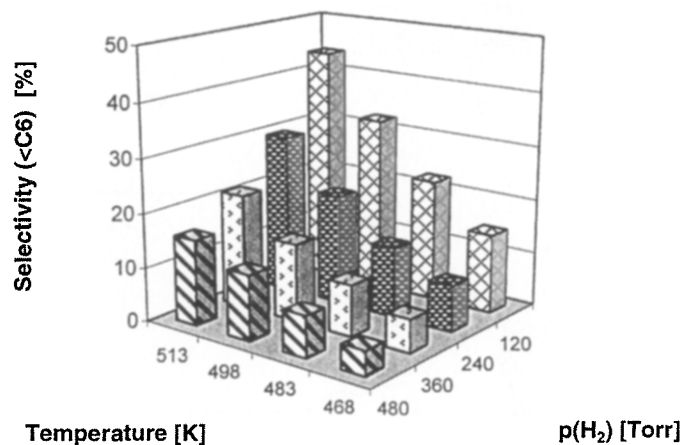


FIG. 5. Fragmentation selectivity as a function of temperature and hydrogen pressure for 3RhHTR.

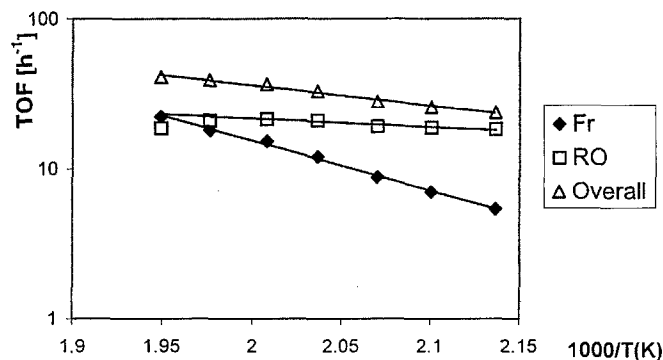


FIG. 6. Arrhenius plots calculated at constant (120 Torr) hydrogen pressure for 0.3RhHTR.

A recent kinetic study (35) reported marked changes (10–120 kJ/mol) in the apparent activation energies for *n*-hexane transformation over EUROPT-1 when the hydrogen order changed from positive to negative values. Since we observed positive and zero hydrogen order only, we concluded that our rather low activation energy values were realistic. The hydrogenolysis activation energies were accompanied with fairly uncertain values for ring opening, due to the Arrhenius plots bending down (Fig. 6). “Bending down” of the Arrhenius plots was observed also in another case (36). Here, it was not caused by the changes in hydrogen order from positive to negative (37) since we were in the positive hydrogen order (Fig. 3) at each temperature. The possible reason may be the change of the prevailing reaction routes. High-temperature reduction resulted in lower activation energies in every case.

The ring opening of MCP occurred “selectively”; i.e., the rupture in the vicinity of the methyl group (position “a”) was strongly hindered (1, 3, 9). Thus, mainly 2-methylpentane (2MP: rupture in position “b”) and 3-methylpentane (3MP: rupture in position “c”) were formed. Figures 7 and 8 show the distribution of ring-opening products (2MP/nH) as a function of temperature and $p(\text{H}_2)$. According to these figures, the catalysts could be divided

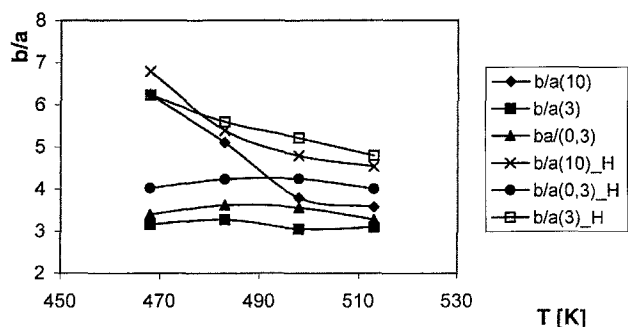


FIG. 7. Ratio of 2MP to nH (b/a) in the ring-opening products as a function of temperature at 480 Torr hydrogen pressure.

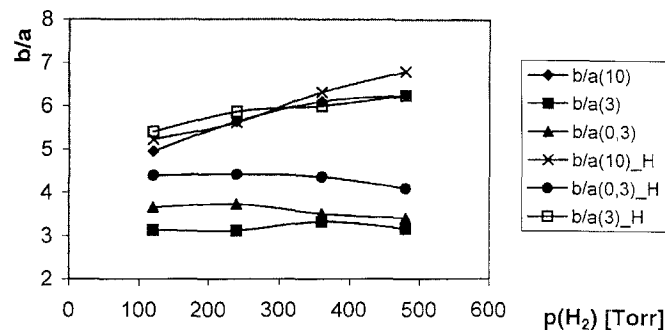


FIG. 8. Ratio of 2MP to nH (b/a) in the ring-opening product distribution as a function of hydrogen pressure at $T = 468$ K.

into two groups. “Group one”: 10Rh and 3RhHTR had higher 2MP/nH ratios, between 3.5 and 7. High hydrogen pressure and low temperature increased the relative importance of 2-methylpentane. “Group two” contained 0.3Rh and 3RhLTR. The 2MP/nH ratios were lower: 3–4.5, independent of temperature and $p(\text{H}_2)$. Both Figs. 7 and 8 suggest that group one catalysts would behave at low $p(\text{H}_2)$ and at higher temperature similarly to group two catalysts, giving low and fairly constant “ b/a ” ratios. High-temperature reduction increased the 2MP/nH ratio in every case. Similar results have been reported in the literature (13, 38).

The probability of breaking the three bissecondary bonds (resulting in two 2MPs plus one 3MP molecule) was rather close to the statistical value of 2. A slight variation of the ratio 2MP/3MP was seen as a function of T and $p(\text{H}_2)$ with group two catalysts, its value being between 1.5 and 1.8. A larger variation was observed with group one catalysts, the values being between 1.4 and 2.3. The probability of the bissecondary bond cleavage, resulting in 2MP, became larger at increased H_2 pressure and decreased temperature.

Hydrogenolysis to fragments—involving multiple rupture of the C–C bonds of the cyclic feed—is another major reaction in addition to ring opening (Table 1). Figure 9 shows the fragment distribution over 3RhHTR at $p(\text{H}_2) =$

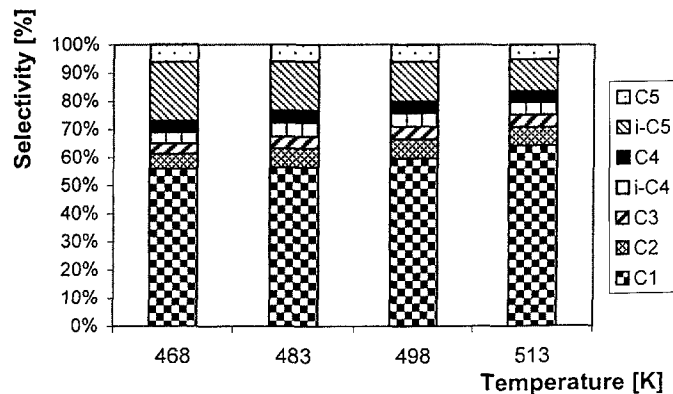


FIG. 9. Fragment distribution obtained over 3RhHTR as a function of temperature at 120 Torr hydrogen pressure. ($\Sigma < C_6 = 100\%$).

120 Torr as a function of temperature. Similar patterns were observed with the other five samples, too. More than 50% of the fragments was methane, its amount increasing with temperature. Another main component was *i*-pentane. Other fragments appeared in similar, low amounts. Higher temperatures decreased the *i*-pentane selectivity accompanied by the already mentioned increase of that of methane. Higher hydrogen pressures had an opposite effect: more *i*-pentane and less methane were formed.

DISCUSSION

Possible Active Forms of the Rh Catalyst

The peak shapes in the first TPR indicated the formation of two types of rhodium in catalysts of different loadings: one formed upon reduction at lower temperature. Its TPR peak was shifted by changing the metal loading. The other was Rh formed upon reduction at high temperature. This high-temperature form was present only in sample 10Rh; therefore, we attribute this form to the production of larger Rh particles. The bimodal particle distribution in the case of 10Rh (as determined by electron microscopy) supports this assumption and will be published separately (39). Oxidation of the reduced catalysts at 873 K for 1 h produced Rh oxide. A subsequent TPR showed that most of the high-temperature form in 10Rh was converted into a low-temperature reduced/oxidized form. This conversion was accompanied by the loss of rhodium reacting with hydrogen, mainly on catalysts with low metal loading. Two forms of Rh can be assumed, following Wong and McCabe (24) who found evidence for two forms of Rh in 1% Rh/SiO₂ catalyst by changing the reduction/oxidation temperature. They observed TPR patterns, after oxidation at 875 K, similar to those of our 10Rh; but with increasing oxidation temperature the relative amount of the high-temperature peak increased until the low-temperature peak appeared as a small shoulder only (oxidation at 1075 K for 2 h). They concluded that (i) there were two types of Rh, a low-temperature oxidized/reduced form and a high-temperature oxidized/reduced form that resembled bulk Rh in its oxidation/reduction behavior, and (ii) interconversion between the two forms occurred readily in alternating oxidizing/reducing environments. Considering our results, these two types of rhodium can arise not only by changing the oxidizing/reducing environments but also by altering the metal loading.

The different types of rhodium behave differently in the hydrogenolytic ring opening of MCP. 10Rh with two TPR peaks had the highest activity. This activity increase can be attributed to larger Rh particles. Both 0.3Rh and 3Rh, showing only one TPR peak, exhibited similar, lower activity. Figures 7 and 8 illustrate this duality in ring-opening product distribution through the presence and absence of the temperature and $p(\text{H}_2)$ effects. The different behav-

iors of 3RhLTR and 3RhHTR reveal that *both* changes in metal loading and pretreatment (24) can cause interconversion between the two forms of Rh. An alternative explanation could be based on the different residual Cl contents of Rh/Al₂O₃ catalysts of various loadings, as concluded from our unpublished XPS studies (39).

Correlation between the Main Catalytic Reactions

High temperature and low hydrogen pressure increased the fragmentation selectivity (Fig. 5). Since we observed only saturated hydrocarbons in the products, the ring opening must have been hydrogenolytic, every C–C bond rupture requiring the uptake of two H atoms. At higher temperature and lower $p(\text{H}_2)$ the degree of the dehydrogenation of the chemisorbed surface intermediate should be higher (2), which results in higher fragment selectivity. The hydrogen effect seen in Fig. 3 suggests that dehydrogenation inhibits ring opening (40). High turnover frequency is attained when the dehydrogenation of the surface intermediate is, likely, low. This can be explained adequately by the earlier assumption concerning associative flat-lying intermediates for selective ring opening (2, 7, 8).

If we consider a common active site for ring opening and fragmentation (the latter being a "secondary" reaction without desorption of the intermediate rather than involving its readsorption), the behavior of apparent activation energies in Table 1 can be explained. When the temperature is low (468 K), the fragmentation is not favorable, but at 513 K the fragment selectivity increases (40%–60%), and the primary ring-opening products "transform" into fragments. This caused the "bending" character of the Arrhenius plots for ring opening (Fig. 6) since these react further at higher temperatures. Fragmentation as a secondary reaction, insignificant at lower temperatures and favored at higher temperature can result in such activation energies (Table 1). A linear correlation between activation energy and the pre-exponential factor is seen in Fig. 10. The single compensation line for the overall and main reactions

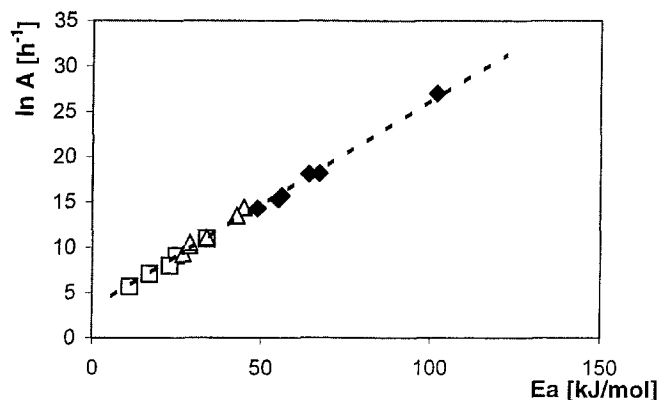


FIG. 10. Compensation line for ring opening (□), for fragmentation (◆), and for the overall reaction (△) at 120 Torr hydrogen pressure.

indicates similar active ensembles according to Bond (41). This result suggests a continuous transformation of the reaction site–intermediate complex, as proposed by Sárkány (42), taking into account the different degree of dehydrogenation deduced previously.

To verify this model (ring opening transforms into fragmentation), we compared the selectivities of *n*-hexane, 3MP, 2MP, and 2MP + fragments in Fig. 11 as a function of temperature and *p*(H₂). Four increasing hydrogen pressures are included at each temperature for the six catalysts. It is important to point out the wide variation in *S*(<C₆) (be-

tween 5% and 60%) and *S*(2MP) (between 20% and 60%). These are very high values; thus, it is quite remarkable that their sum is relatively constant ($\pm 10\%$). Two different behaviors are observed: (i) there are catalysts where the selectivities (*n*H, 3MP, 2MP + <C₆) are independent of the reaction conditions (Figs. 11d–11f) and (ii) there are samples where a clear variation is shown (Figs. 11a–11c). Of the second group (“group two”), 0.3RhLTR (11a) can be selected as an example. *S*(*n*H), *S*(3MP), and *S*(2MP) change in a parallel way: higher temperature and lower hydrogen pressure decrease their selectivities. This decrease is accompanied

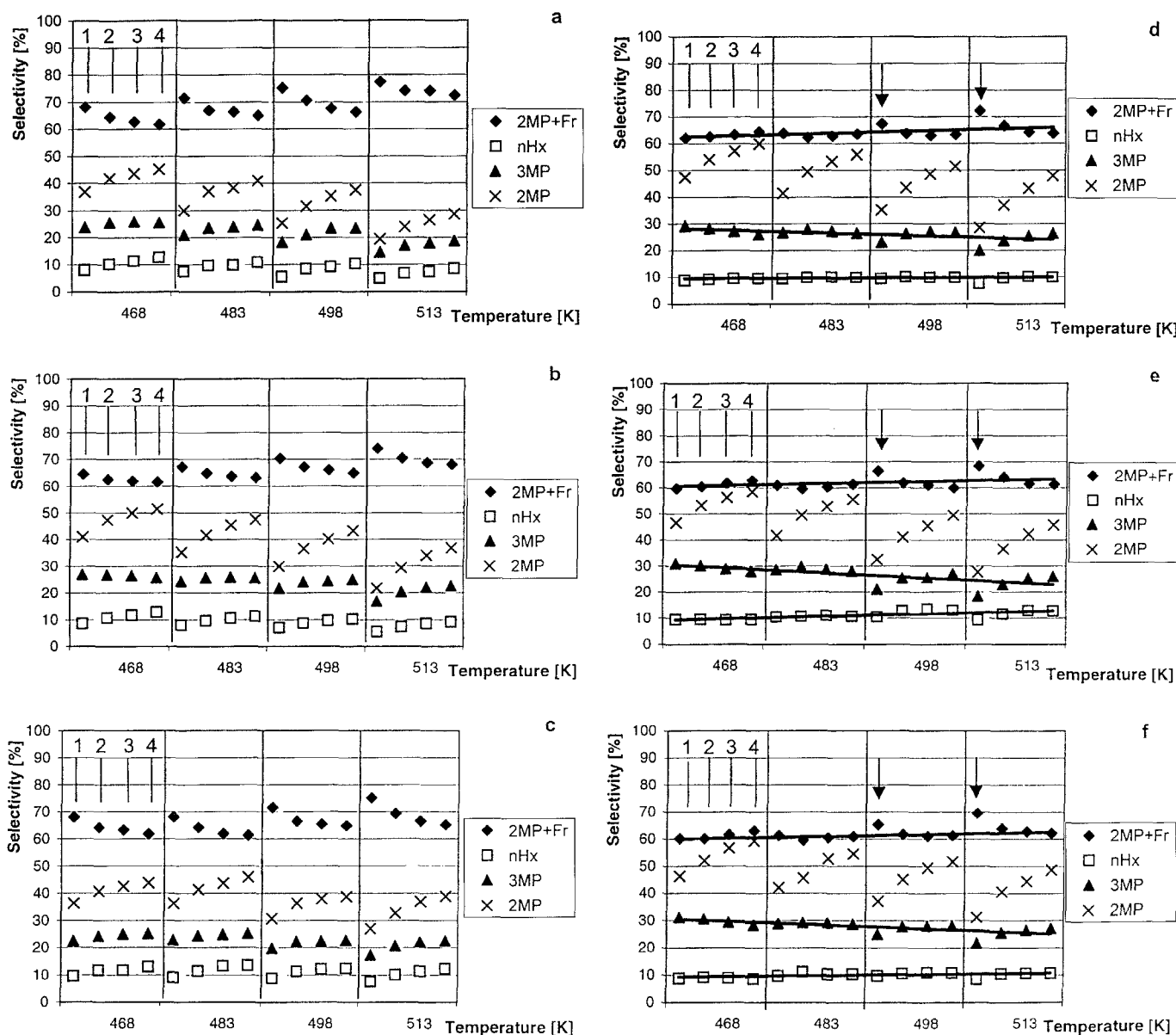


FIG. 11. Selectivity comparison for *n*-hexane, 2-methylpentane, 3-methylpentane, and 2-methylpentane + fragments (a. 0.3RhLTR, b. 0.3RhHTR, c. 3RhLTR, d. 3RhHTR, e. 10RhLTR, and f. 10RhHTR). Each temperature includes four increasing hydrogen pressures abbreviated as follows: 1. 120 Torr, 2. 240 Torr, 3. 360 Torr, and 4. 480 Torr. They are shown at the lowest temperature, for clarity.

by the opposite changing of $S(2MP + <C_6)$. Somewhat different behaviors can be observed with the other three samples. Figure 11f shows constant selectivities (with the exception of 2MP) for the two lower temperatures and this statement is almost valid for the whole temperature range if we leave out the points denoted by arrows. These points represent measurements where the fragmentation selectivity was the highest. The changing $S(3MP)$ and $S(nH)$ here and their constant values observed elsewhere reveals that fragments were mainly produced—with the exception of the signed points—after opening the ring in position b and by subsequent C–C bond ruptures before desorption. Similar complementary behavior between fragments and 2MP was reported by other authors (14–17). (Surprisingly, Anderson and Burch (15) found lower fragmentation selectivity at higher temperatures.) The fragment distribution from the 2MP feed (9, 39) was similar to the present results (see Fig. 9), and this also supports the previous model.

The different temperature responses (Fig. 7) can also be explained. The decrease of the 2MP/nH ratio as a function of temperature for group one Rh catalysts was the result of the increasing fragmentation selectivity with temperature. This selectivity increase was accompanied by the parallel decrease of the amount of 2MP. The $S(nH)$ being, at the same time, constant; thus, the ratio “b/a” decreased. The same explanation can be given for the hydrogen effect (Fig. 8). In the case of the group two catalysts the lack of T and $p(H_2)$ effects (Figs. 7 and 8) could be caused by the random secondary fragmentation (Figs. 11a–11c) of the ring-opening surface species. Hydrogenolysis products were formed in a random way at the expense of ring-opening products.

Since both the ring-opening and the fragmentation distribution changed with T and $p(H_2)$, we can attempt to correlate the two distributions to obtain further information about the proposed common surface intermediate. The formation of pentanes can be explained by breaking two C–C bonds during one sojourn of the feed molecule on the active ensemble. Such a simultaneous breaking in positions b and c results in an isopentane fragment. *n*-Pentane, in turn, is produced by breaking C–C bonds in positions b and a. Due to the hindered single rupture in position a, less *n*-pentane can be formed. The suggestion that the same rule is valid for the reactions leading to one or two C–C bond rupture(s), respectively, is illustrated by Fig. 12, comparing the ratio of the iC_5/nC_5 with that of the 3MP/*n*-hexane. The use of the ratio of C_5 products is simpler in the case of the cyclic reacting molecule than considering other fragments, too (43, 44). A loose positive correlation has been observed between the c/a ratio and the iC_5/nC_5 ratio in the case of the first group of catalysts (10Rh, 3RhHTR). It indicates that the same active sites may be responsible for the formation of C_5 and C_6 alkanes. The surface intermediate retained its geometry after the first C–C bond rupture, which is necessary to

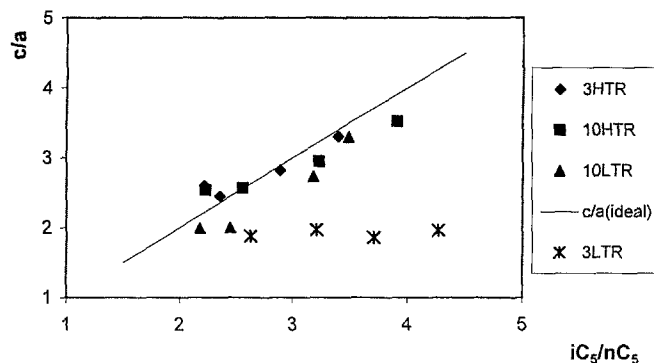


FIG. 12. Correlation between the ratio of 3-methylpentane to *n*-hexane (c/a) in the ring-opening products and the C_5 fragment ratio (iC_5/nC_5). Results obtained at 120 Torr hydrogen pressure are shown for clarity. Data obtained at each temperature are included. The straight line represents the ideal case of $c/a = iC_5/nC_5$.

obtain such a correlation. A similar relationship between those two ratios was reported in our previous work (12) and can be found in McCarthy *et al.*'s (17) data. In the case of the second group (0.3Rh, 3RhLTR) the parallel changes in the ring-opening products while the fragmentation selectivity is altered result in a constant 3MP/nH ratio. However, the variation in the ratio iC_5/nC_5 is still observed. The flat-lying geometry (1, 2, 7) with the governing effect of the Rh (selective mechanism for C–C cleavages) can satisfactorily explain the correlation mentioned previously.

Foger and Anderson (45) distinguished two “archetypal” behaviors for an alkane reacting on a metal catalyst: the “ C_2 -mode” reactivity would involve primary and secondary C atoms only whereas reactions of tertiary C atoms would proceed according to the “iso-mode”. Garin and Maire (43, 44) calculated the ratio of the two reaction modes on the basis of the ratio of different fragments produced from 2MP over several metal catalysts. The iso-mode reaction prevailed on Pt, Pd, and Ni, but it was minor on Ir, Ru, and its alloys. Methylpentanes as well as isopentane from MCP would be produced by the C_2 mode reaction. This route prevailed thus on Rh, too, like on Ru and Ir (43). These properties may be correlated with the electronic effect of these metals being most important to determine the main reaction mode (43, 44).

CONCLUSIONS

The main conclusions of this work can be summarized as follows:

1. Alumina-supported rhodium shows a “selective” ring-opening mechanism for MCP (9, 12). The variation in the ring-opening product distribution as a function of T and $p(H_2)$ was caused by the different abilities of the ring-opening surface intermediates to react further in hydrogenolysis.

2. The results in this study are in agreement with earlier assumptions (2, 7, 8) that selective ring opening involves an associative flat-lying intermediate. According to our interpretation, this intermediate can be a common surface intermediate for single- and multiple-C–C bond cleavage.

3. TPR indicated the presence of two forms of rhodium. Their different behaviors in MCP ring opening is obvious. Whereas group one (10Rh, 3RhHTR) showed strong *T* and *p*(H₂) dependence in the ring-opening product distribution, caused by the favored fragmentation of 2MP, group two (0.3Rh, 3RhLTR) catalysts exhibited random fragment production from each ring-opening surface species.

4. Changes in metal loading (0.3 ↔ 10%Rh) and pretreatment (3RhLTR ↔ 3RhHTR) can cause interconversion between the two forms of Rh, as shown by the respective catalytic results. Since the changes in TPR and catalytic behavior with metal loading and pretreatment were parallel, we attribute the changes in product distribution to different morphologies of Rh particles.

ACKNOWLEDGMENTS

We are indebted to D. Duprez for helpful discussions and encouragement. Financial support from the Hungarian National Science Foundation Grant OTKA T25599 is gratefully acknowledged.

REFERENCES

- Paál, Z., and Tétényi, P., *Nature* **267**, 234 (1977).
- Paál, Z., and Tétényi, P., in "Catalysis Specialists Periodical Reports" (G. C. Bond and G. Webb, Eds.), Vol. 5, p. 80. The Chemical Society, London, 1982.
- Maire, G., Plouidy, G., Prudhomme, J. C., and Gault, F. G., *J. Catal.* **4**, 556 (1965).
- Kramer, R., and Zuegg, H., *J. Catal.* **80**, 446 (1983).
- Kramer, R., and Zuegg, H., in "Proceedings, 8th International Congress on Catalysis, Berlin, 1984," Vol. 5, p. 275. Dechema, Frankfurt-am-Main, 1984.
- Barron, Y., Maire, G., Muller, J. M., and Gault, F. G., *J. Catal.* **5**, 428 (1966).
- Zimmer, H., and Paál, Z., *J. Mol. Catal.* **51**, 261 (1989).
- Bragin, O. V., and Liberman, A. L., *Usp. Khim. (Russ. Chem. Rev.)* **39**, 2122 (1970).
- Del Angel, G., Coq, B., Dutartre, R., and Figueras, F., *J. Catal.* **87**, 27 (1984).
- Schepers, F. J., van Senden, J. G., van Broekhoven, E. H., and Ponec, V., *J. Catal.* **94**, 400 (1985).
- Fenoglio, R. J., Nunez, G. M., and Resasco, D. E., *J. Catal.* **121**, 77 (1990).
- Teschner, D., and Paál, Z., *React. Kinet. Catal. Lett.* **68**, 25 (1999).
- Fülöp, E., Gnutzmann, V., Paál, Z., and Vogel, W., *Appl. Catal.* **66**, 319 (1990).
- Coq, B., Dutartre, R., Figueras, F., and Tazi, T., *J. Catal.* **122**, 438 (1990).
- Anderson, J. B. F., and Burch, R., *J. Chem. Soc. Faraday Trans.* **83**, 913 (1987).
- Dumas, J. M., Géron, C., Hadrane, H., Marécot, P., and Barbier, J., *J. Mol. Catal.* **77**, 87 (1992).
- McCarthy, T. J., Lei, G.-D., and Sachtler, W. M. H., *J. Catal.* **159**, 90 (1996).
- Kalakkad, D., Anderson, S. L., Logan, A. D., Peña, J., Braunschweig, E. J., Peden, C. H. F., and Datye, A. K., *J. Phys. Chem.* **97**, 1437 (1993).
- Sadi, F., Duprez, D., Gérard, F., Rossignol, S., and Miloudi, A., *Catal. Lett.* **44**, 221 (1997).
- Lee, C., and Schmidt, L. D., *J. Catal.* **101**, 123 (1986).
- Gao, S., and Schmidt, L. D., *J. Catal.* **111**, 210 (1988).
- Rupprechter, G., Hayek, K., and Hofmeister, H., *J. Catal.* **173**, 409 (1998).
- Rupprechter, G., Seeber, G., Goller, H., and Hayek, K., *J. Catal.* **186**, 201 (1999).
- Wong, C., and McCabe, R. W., *J. Catal.* **107**, 535 (1987).
- Dobrovolszky, M., Matusek, K., Paál, Z., and Tétényi, P., *J. Chem. Soc. Faraday Trans.* **89**, 3137 (1993).
- Kip, B. J., Duivenvoorden, F. B. M., Koningsberger, D. C., and Prins, R., *J. Catal.* **105**, 26 (1987).
- Martin, D., and Duprez, D., *Appl. Catal.* **131**, 297 (1995).
- Guerrero-Ruiz, A., Bachiller-Baeza, B., Ferreira-Aparicio, P., and Rodríguez-Ramos, I., *J. Catal.* **171**, 374 (1997).
- Vis, J. C., Van't Blik, H. F., Huizinga, T., Van Grondelle, J., and Prins, R., *J. Mol. Catal.* **25**, 367 (1984).
- Delahay, G., and Duprez, D., *J. Catal.* **115**, 542 (1989).
- Yao, H. C., Japan, S., and Shelef, M., *J. Catal.* **50**, 407 (1977).
- Paál, Z., in "Hydrogen Effect in Catalysis" (Z. Paál and P. G. Menon, Eds.), p. 449. Marcel Dekker, New York, 1988.
- Paál, Z., and Menon, P. G., *Catal. Rev.-Sci. Eng.* **25**, 223 (1983).
- Bond, G. C., Coq, B., Dutartre, R., Ruiz, J. G., Hooper, A. D., Proietti, M. G., Sierra, M. C. S., and Slaa, J. C., *J. Catal.* **161**, 480 (1996).
- Wootsch, A., and Paál, Z., *J. Catal.* **185**, 192 (1999).
- Davis, S. M., Zaera, F., and Somorjai, G. A., *J. Catal.* **85**, 206 (1984).
- Paál, Z., *J. Catal.* **91**, 181 (1985).
- Hayek, K., Kramer, R., and Paál, Z., *Appl. Catal.* **162**, 1 (1997).
- Teschner, D., Paál, Z., Labruquere, S., Duprez, D., Wild, U., and Schlögl, R., in preparation.
- Paál, Z., *Catal. Today* **2**, 595 (1988).
- Bond, G. C., *Z. Phys. Chem. N. F.* **144**, 21 (1985).
- Sárkány, A., *J. Mol. Catal.* **51**, 239 (1989).
- Garin, F., and Maire, G., *Acc. Chem. Res.* **22**, 100 (1989).
- Garin, F., and Maire, G., *J. Mol. Catal.* **52**, 147 (1989).
- Foger, K., and Anderson, J. R., *J. Catal.* **59**, 325 (1979).